

Biomechanical surface roughness analysis of ramie-low melt polyester nonwovens exposed to plasma

Markus Paramahasti¹, Valentinus Galih Vidia Putra², Yusril Yusuf³

^{1,3}Department of Physics, Universitas Gadjah Mada, Yogyakarta, Indonesia

²Basic and Applied Science Research Group in Theoretical and Plasma Physics, Department of Textile Engineering, Politeknik STTT Bandung, Bandung, Indonesia

³Corresponding author

E-mail: ¹markus.paramahasti@mail.ugm.ac.id, ²valentinus@kemenperin.go.id, ³yusril@ugm.ac.id

Received 15 January 2024; accepted 6 June 2024; published online 22 August 2024

DOI <https://doi.org/10.21595/jme.2024.23933>



Copyright © 2024 Markus Paramahasti, et al. This is an open access article distributed under the Creative Commons Attribution License, which permits unrestricted use, distribution, and reproduction in any medium, provided the original work is properly cited.

Abstract. This study aims to characterize ramie-low melt polyester nonwoven fabrics treated with low-temperature plasma and to analyze 3-D images based on object-depth mapping (ODM) using the MATLAB® R2022a software. We examined the low-temperature plasma treatment of nonwoven ramie fabrics using a plasma generator with 30 kV output power, six-minute treatment times, and a 4.5 cm distance between electrodes. The fabric's chemical properties and surface topography were investigated using scanning electron microscopy (SEM) and infrared spectroscopy (FTIR). An analysis of the SEM images was performed using a statistical approach and image processing to determine the level of surface roughness. FTIR analysis revealed that fabrics exposed for six minutes differed from those that were not. Our findings indicated that plasma treatment caused the following: 1) Ramie fabrics to become more hydrophilic, as shown by their increased T% in the FTIR of hydrophilic functional groups such as hydroxyl (O-H), carboxyl (-COOH), and carbonyl (C=O); 2) A higher surface roughness was observed in nonwoven fabric during SEM testing and image processing; 3) Plasma treatment of fabrics resulted in a higher coefficient of variation (CV) than untreated fabrics; 4) Nonwoven fabric mass reduction. Based on this study, we found the relationship between plasma-treated ramie fabric and textiles in biomechanics. Plasma treatment reduced the mass of ramie fabric by 0.11 %, according to our findings. We found that the greater the mass reduction, the greater the surface roughness value. The novelty of this study is the use of 3-D images based on object-depth mapping (ODM) using the MATLAB® R2022a software in SEM to observe surface roughness to the physical properties of ramie fabric for the first time.

Keywords: ramie fiber, ramie nonwoven, plasma treatment, nonwoven characterization, mathematical model.

1. Introduction

Since natural fibers are readily available in nature, affordable, biodegradable, and lightweight, they are increasingly used as composite reinforcement. The flexibility and elastic properties of cellulose fibers enable them to maintain high aspect ratios during manufacturing compared with mineral fibers such as glass and carbon fibers [1, 2]. Due to the growing awareness of environmental issues and new environmental regulations, materials derived from renewable resources, such as natural cellulosic fibers, are attracting increasing interest. Typically, natural cellulosic fibers contain varying amounts of cellulose, hemicellulose, and lignin. These fibers are composed primarily of cellulose, which is bundled into usually connected bundles [3-5]. The ramie fiber is among the most widely used lignocellulosic fibers in polymer composites because of its high crystallinity and commercial availability [6-8]. In addition to being the longest and strongest fine textile fiber, a ramie fiber consists of a single-cell structure whose diameter and length range from 11 to 80 μm and 60 to 250 mm, respectively [9]. The walls of cells are composed of oriented semi-crystalline cellulose molecules with diameters of a few nanometers embedded in an amorphous matrix of lignin and non-cellulose compounds such as hemicellulose

and pectin. Despite its many benefits and potential, the use of ramie fibers is limited by some problems. Since ramie fibers are hydrophilic, they cannot adhere to hydrophobic polymer matrixes [10-13]. To address this issue, ramie fibers can be surface-modified to become more hydrophobic. There have been several surface modification techniques used in the past, including alkaline treatments [14-17], acetylation treatments [18, 19], and stearic acid treatments [19, 20]. Interfacial adhesion has been demonstrated to be improved by some of these treatments. Nevertheless, there are still problems related to the disposal of polluted waste, the high consumption of energy and water, and damage to fibers. Plasma treatment is a more environmentally friendly and practical method of modifying fiber surfaces, as it alters a surface's chemical and physical properties without affecting its bulk properties [21]. Plasma comprises free particles and is the fourth state of matter after solids, liquids, and gases. Some studies have demonstrated that corona discharge plasma can effectively improve the adhesion properties of textile materials (e.g., woven, knitted, and nonwoven fabrics) [22-24]. Plasma sources have been extensively researched as a substitute for conventional wet chemical methods of surface modification of polymers [22, 23]. In biomechanics, some researchers reported a relationship between plasma-treated fabric and textiles. Three key points: (1) Tensile Strength: Plasma treatment increases tensile strength, which is important for biomechanical products like sportswear; (2) Light and strong: Plasma treatment keeps the fabric light but strong, allowing for natural body movement; and (3) Moisture Control: Plasma-treated fabric soaks up moisture and encourages air circulation, which enhances comfort in biomechanical product design [22-24]. The use of plasma for modifying polymers has been reported by some researchers [23-29], for example, to improve adhesion and surface roughness. The work of adhesion of a material can be enhanced using the plasma treatment technique [30]. Plasma treatment also can be used to modify the electromagnetic properties of a fabric [31]. The effects of plasma treatment on ramie fibers have been investigated in previous studies [6, 13, 32]. Some studies of plasma treatment on ramie composite have also been conducted by some researchers [13, 32]. Researchers have traditionally examined the plasma treatment effect on fibers using the scanning microscope electron method. However, the analysis of scanning electron microscopes has not been conducted using image processing. In addition, quantitative measurements of surface roughness cannot be made based on SEM images directly. The analysis of two-dimensional and three-dimensional images has been demonstrated to be useful for studying surface roughness by some researchers [33-38]. However, nonwoven fiber's surface roughness on microscopic scales is more difficult to measure directly [36, 39]. There are several advantages to the three-dimensional image processing analysis technique, including the absence of physical contact, the lack of surface material damage, and ease of implementation [33]. This study aimed to investigate surface roughness for nonwoven fabric made from ramie fiber with FTIR chemical structure using image processing in SEM for the first time. The effects of corona plasma treatment on ramie-low melt polyester nonwoven fabrics were investigated using infrared spectroscopy and three-dimensional image processing analysis. The significance of ramie material research and its application in the biomedical and biomaterial fields originates from the fact that ramie fiber is a good choice for use in medical products such as dressings and bandages due to its strength and durability. Its resistance to stress while remaining strong may be useful in these products. In some cases, natural fibers such as ramie may be used as a potential material for medical implants. Ramie fiber's durability, biocompatibility, and specific strength properties can be used to develop potential implant materials [40]. In this study, the nonwoven fabrics were treated using a corona plasma apparatus with 25 electrode tips and a flat electrode. SEM, FTIR, and three-dimensional image analysis were used to study the modification effect. The novelty of this study is the use of 3-D images based on object-depth mapping (ODM) with the MATLAB® R2022a software in scanning electron microscopy to observe surface roughness and its relationship to the physical properties of the ramie fabric for the first time. This research also aims to investigate the physical properties of ramie fabrics before and after plasma treatment. Scientists and engineers can use the findings in this study to improve the quality of nonwoven fabrics by using environmentally friendly methods.

2. Research methods

2.1. Materials

In this study, we used ramie fibers (*Boehmeria Nivea L. Gaud*) purchased from CV Rabersa in Wonosobo, Central Java, Indonesia. The polymer matrix was made from a low-melt polyester resin obtained from Politeknik STTT Bandung, Indonesia. The nonwoven fabric was made using a hot press machine with a grammage of 50 grams/30 cm², 40 grams of ramie fiber, and 10 grams of low-melt polyester. The ratio between ramie fiber and polyester binder was 80:20, and the size of the fabric sample was 30×30 cm². After decomposing and weighing the fibers, the cotton selector tool was used to mix the fibers evenly. In the hot press machine, fibers were pressed for 30 seconds at 150 degrees and a pressure of 100 bars after mixing.

2.2. Instrumentation

As part of this study, a prototype apparatus, low-temperature plasma (corona plasma), was assembled in the Physics Laboratory of Politeknik STTT Bandung, the Ministry of Industry of the Republic of Indonesia. The corona plasma generator had an electrode configuration, a multi-tip, and a flat electrode connected to a power source. The plasma generator used twenty-five tipped bolts as the multi-tip electrode. This multi-tip electrode was used as a positive electrode perpendicular to the flat electrode. A high-voltage multi-tester (ISO 16750-2) was used at the Physics Laboratory of Politeknik STTT Bandung to measure the D.C. and A.C. input voltages. The experimental design and instruments used in this study are illustrated in Fig. 1. We also measured the mass of the nonwovens with a micro-analytical balance during this study.

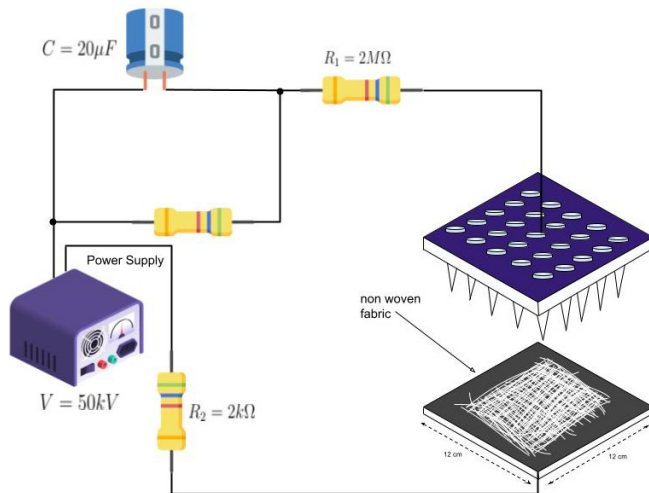


Fig. 1. Design of corona plasma generator used in the research

2.3. Scanning electron microscopy

A scanning electron microscope (SEM) JEOL JSM-6360LA with an energy dispersive system (EDS) was used at the Marine Geological Research and Development Center, Bandung, Indonesia, to examine the surface morphology of ramie fibers.

2.4. Fourier transform infrared spectroscopy

The chemical composition of fibers was analyzed using a Shimadzu Prestige 21 FTIR apparatus in the Physics lab at the Faculty of Mathematics and Natural Science, ITB, Indonesia.

The FTIR analysis was conducted between wavenumber frequencies of 4000 and 500 cm^{-1} . We did not perform signal correction to avoid data loss.

2.5. Experimental methods

A scanning electron microscope (SEM) and infrared spectroscopy (FTIR) were used to investigate the effects of corona plasma treatments on nonwoven fabric. Fig. 2 illustrates the experimental design and instruments in this research. For the application of plasma to the nonwoven samples, a flat electrode was used in the chamber. We adjusted the voltage to 30 kV, the plasma exposure time to 6 minutes, and the electrode distance to 4.5 cm for this study. Fig. 2 shows the plasma treatment of nonwoven fabric. FTIR and SEM were used to characterize the nonwoven fabrics after exposure to plasma at room temperature and atmospheric pressure. The mass of plasma-treated nonwoven fabric was also measured before and after plasma treatment to investigate the effect of plasma treatment on the fabric.

2.6. Image processing

An approach to obtaining the 3D effect from a single photograph is described here. Based on the object-depth mapping, different depth levels of an object were encoded with different color intensities. As a result of this process, a 3D image stack was created. This study is a simple principle underpinning one-photograph stereo-imaging: object-depth mapping. A brighter object appeared closer to the viewer, while a darker object appeared further away. An object's color map was created by assigning brightness and darkness values to color codes. In the end, an image stack was produced from each color code. According to a well-defined procedure, this stack made the 3D image. We analyzed the SEM images obtained during the experiment. Our study demonstrated that SEM images could be used to visualize three-dimensional images based on object-depth mapping. A MATLAB program created histograms and analyzed the images' morphology in three dimensions. Once the three-dimensional image had been obtained, a histogram was generated to see the pixel intensity distribution of the images. An analysis of the images is performed in the following manner: 1) collecting the original SEM image; 2) converting the images into grayscale; 3) analyzing the grayscale histogram; 4) generating a three-dimensional surface plot; 5) calculating the mean of all array values; and 6) calculating the standard deviation, mean, standard error, and coefficient of variation. The statistical variables of the data, such as the standard deviation (σ), mean (μ), standard error (SE), and coefficient of variation (CV) for indicating surface roughness were calculated according to Eqs. (1) to (5).

$$\sigma = \sqrt{\frac{\sum_i (x_i - \mu)^2}{N - 1}}, \quad (1)$$

$$\mu = \frac{\sum_i x_i}{N}, \quad (2)$$

$$SE = \frac{\sigma}{\sqrt{N}} \quad (3)$$

$$CV = \frac{\sigma}{\mu} \quad (4)$$

$$grayscale = 0.299 \times R + 0.587 \times G + 0.114 \times B, \quad (5)$$

where x_i represents grayscale pixel intensity (0-255) and image dimension; N is the number of pixels; SE is the standard error; and CV is the coefficient of variation. A higher CV value indicates irregular fibers of fabrics. CV value is calculated as the ratio of the standard deviation of mass variation divided by the average mass variation. The color spectrum is made up of the tristimuli R (red), G (green), and B (blue). Using the NTSC equation provided by MATLAB, the following

RGB values are converted to grayscale: $0.299 \times R + 0.587 \times G + 0.114 \times B$. The resulting equation accurately represents the average individual's perceived brightness of red, green, and blue light. According to Eqs. (6) to (8), the R, G, and B components can be obtained using three color filters with different radiances and wavelengths: the red filter S_R , the green filter S_G , and the blue filter S_B :

$$R = \int L(\lambda)S_R d\lambda, \quad (6)$$

$$G = \int L(\lambda)S_G d\lambda, \quad (7)$$

$$B = \int L(\lambda)S_B d\lambda. \quad (8)$$

As we can see in Eqs. (6) to (8), R, G, and B components aren't independent but are actually correlated. In this study, $R = G = B = (0-255)$ represents the gray level from black to white in the RGB color space.

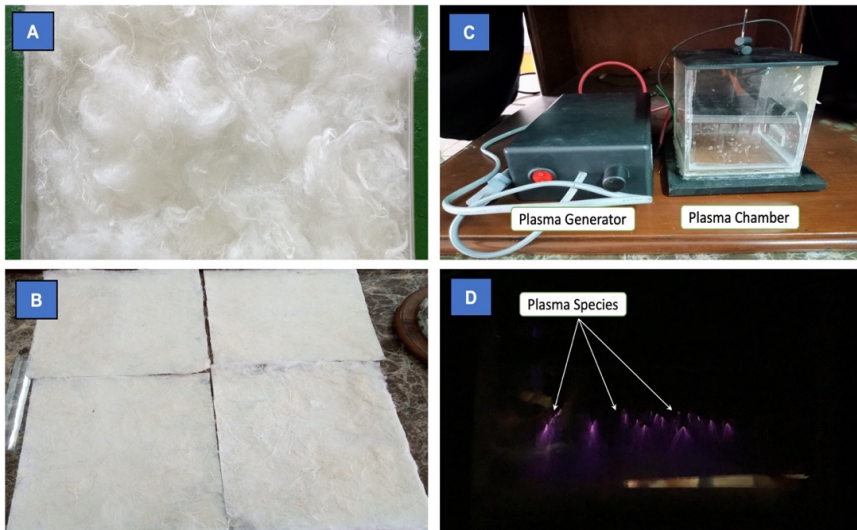


Fig. 2. The experimental design and instruments in this research: a) ramie fibers mixed with low melt polyester, b) ramie nonwoven fabrics (30 cm×30 cm), b) corona plasma apparatus, d) plasma treatment process

3. Results and discussions

3.1. Infrared spectroscopy analysis

An FTIR spectrometer was used at room temperature and atmospheric pressure to measure surface modifications caused by atmospheric plasma treatment. FTIR spectroscopy was used to identify and quantify the chemical bonds between the untreated and plasma-treated fabric. Fig. 3 shows the infrared spectra of untreated and plasma-treated fibers and some characteristics of their absorption peaks. The treated fibers (fabric with six minutes plasma exposure time) were virtually transformed compared to untreated fibers. Therefore, the chemical groups of the fabric have changed due to this plasma treatment. Fig. 3 illustrates some chemical bond changes in fabric treated by plasma. Several absorption bands were observed in the infrared spectrum of nonwoven fabrics, including cellulose, hemicellulose, lignin, waxes, and water. The infrared spectrum of the fabrics showed some peaks that were indicative of their chemical composition. The C-O-C

stretching mode, a component of the cellulose structure, was visible at wavenumber 2126 cm^{-1} . We found that O-H stretching occurred at wavenumber 3427 cm^{-1} . The C=O and C-O stretching modes were also observed at wavenumbers 1721 cm^{-1} and 2126 cm^{-1} . At the wave number spectrum, 1721 cm^{-1} , it could be the C=O stretching mode from aromatic ester in the polyester structure in the fabrics. In Table 1, the significant bands are summarized in terms of their attributes. According to the infrared spectra, plasma-treated transmittance (T%) was generally lower than untreated transmittance (T%). It was possible to achieve this result because of the plasma reaction between the fabric surface and the plasma species provided by the treatment. It can be seen from Fig. 3 that transmittance dropped from 41 % to 21 % at wavenumber 3427 cm^{-1} . There was a decrease in T% at wavenumber 3427 cm^{-1} , corresponding to O-H stretching due to the interaction between the fabric surface and the plasma species. The plasma-treated fabric had a lower transmittance (T%) at 1641 than the untreated fabric. This reaction likely resulted in removing fatty acids and waxes in the plasma-treated fabric. A deeper transmittance (T%) was observed in FTIR after plasma treatment of fabric, indicating that hydrophilic functional groups such as hydroxyl (O.H.), carboxyl (O.C.), and carbonyl (C=O) were present in the fabrics.

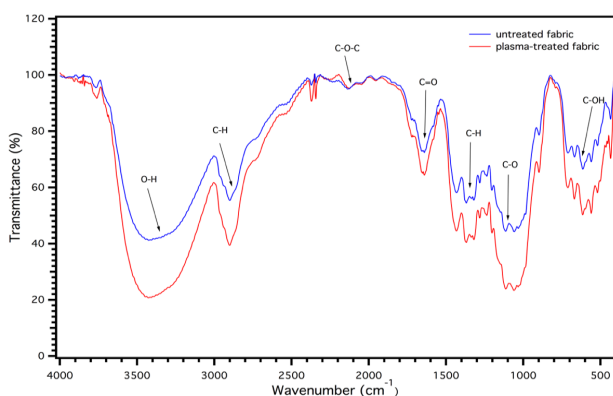


Fig. 3. FTIR spectra of untreated and plasma-treated nonwoven fabric

Fig. 3 shows FTIR spectra for untreated and atmospheric plasma-treated samples. The plasmatreated sample contains additional hydroxyl groups (oxygen that is single bonded to carbon and single bonded to hydrogen) as evidenced by a sharp absorption band with peak intensity at 3427 cm^{-1} , which is characteristic of C-OH. The wettability of a sample increases with the increase in hydroxyl groups on the sample. A distinct FTIR peak was also observed at 1113 cm^{-1} , characteristic of the C-O peak in plasma-treated samples, which were significantly higher than in untreated samples, indicating the presence of acidic groups. Carboxyl groups are formed by bonding two oxygen atoms to a carbon atom, as we discovered. The two oxygen atoms have a double bond (C=O), and the other oxygen atom has a hydrogen bond (-C-OH). Carboxyl groups are represented by the symbol -COO-H. In addition, treated fabric had a higher peak in Carboxyl groups than untreated fabric. The greater the number of double bonds formed, the stronger the bonds between the molecules. Based on the FTIR spectrum of the treated fabric, functional group grafting may be responsible for the higher peak. The plasma treatment of the fabric surface resulted in new functional groups (e.g., -O.H. and -COOH), which affected wetting time and facilitated graft polymerization. The FTIR spectra of treated fabric revealed hydrophilic functional groups, including hydroxyl, carbonyl, and carboxyl groups. In the volume between the electrodes, electrons can be separated from atoms and molecules with sufficient energy. Electrons and ions on a surface determine its ability to modify the fabric surface. In our study, we found that plasma species become more active at higher voltages (as indicated by FTIR analyses of fabric samples for high levels of hydroxyl groups, carbonyl groups, and carboxyl groups), and the more active

the plasma species, the greater the modification of the fabric surface. The results of the present study are also consistent with those reported by some researchers who have used plasma to change polymers, for example, adhesion, chemical structure, and surface roughness [20-25, 41].

Table 1. Summary of observed FTIR absorption peaks for ramie fabric with associated chemical components

Peak wavenumber (cm ⁻¹)	Relative bonding	Associated chemical component
3427	O-H stretching	Cellulose
2901	C-H stretching	Cellulose and hemicelluloses
2126	C-O-C stretching	β – glucoside linkage
1721	C=O stretching	Cellulose, hemicelluloses, aromatic ester
1641	O-H bending	Hydroxyl and cellulose
1433	C-H deformation	Lignin
1319	O-H deformation	Lignin
1234	C-O stretching	Waxes
1113	C-O stretching	Cellulose and Lignin
669	C-OH bending	Lignin

3.2. Surface morphology analysis

Plasma treatment improved the surface properties of ramie fabric, especially the roughness. As shown in Fig. 4, our visual examination of plasma-treated ramie fabric using scanning electron microscopy (SEM) indicates that the surface roughness of the plasma-treated fabric is greater than the surface roughness of the untreated fabric. Fig. 4(a) shows the untreated ramie fabric, and Fig. 4(b) shows the plasma-exposed fabric. The result from the SEM investigation seems to be that plasma-treated fabrics have better roughness. Fig. 4(b) shows that the fabric fiber has many scratches compared to Fig. 4(a). In this study, we found that plasma treatment reduced the mass of ramie fabric by 0.11 %. The roughness of the surface was measured quantitatively using image processing. MATLAB® R2022a was used to simulate the SEM images.

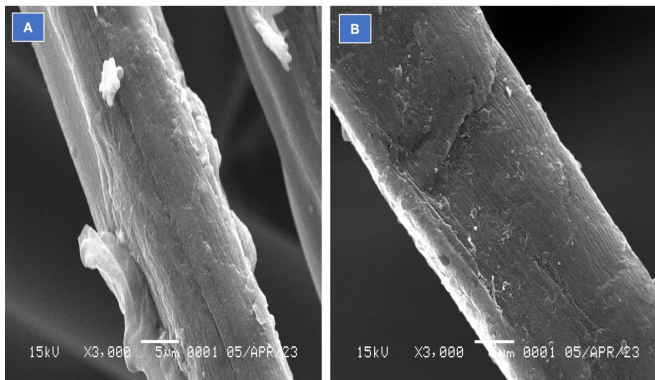


Fig. 4. SEM images comparison: a) untreated fabric and b) plasma-treated fabric

Fig. 5 illustrates the three-dimensional plot of the SEM images. In Fig. 5, the *x* and *y* axes represent the pixel size, while the *z*-axis represents the pixel intensity (0-255). Fig. 5(a) shows the three-dimensional image processing of the SEM image of the untreated ramie fabric, and Fig. 5(b) shows the three-dimensional image processing of the SEM image of the plasma-exposed fabric. According to these results, the intensity of pixels is more evenly distributed throughout the plasma-exposed fabric than it is in the untreated fabric. Fig. 6 depicts the relative frequency distribution of pixel intensity, and Table 2 summarizes the statistical results. Fabric that has been treated with plasma had a higher coefficient of variation, 0.6326, than fabric that has not been treated with plasma. This result indicates that plasma-treated fabric is rougher than untreated

fabric. We found that the fabric mass also decreased due to the plasma treatment process. The fabric mass was 4.2146 ± 0.3413 grams before and 3.7319 ± 0.3413 grams after the treatment. Reactions of plasma species with fabric surfaces resulted in a mass reduction of 0.11 %. The fabric surface was etched and cleaned through the plasma reaction, reducing its mass.

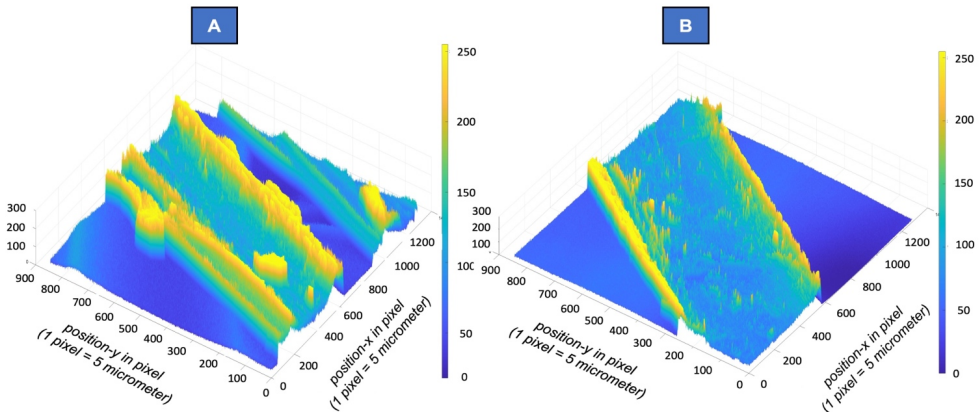


Fig. 5. Three-dimensional SEM using image processing: a) untreated fabric and b) the plasma-treated fabric

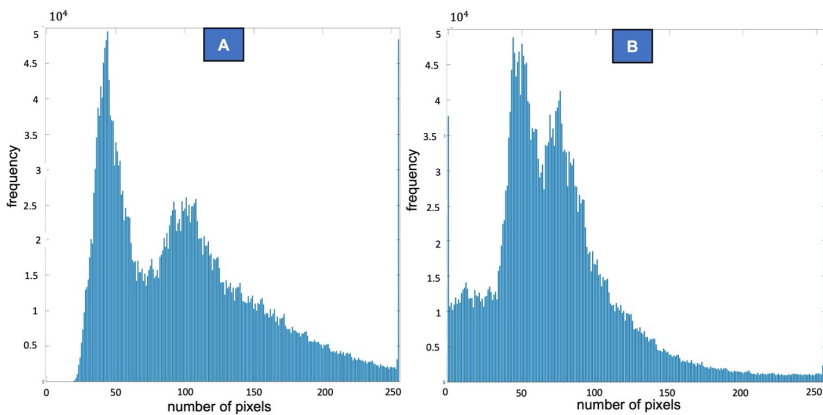


Fig. 6. Histogram of the pixel intensity comparison from SEM using image processing: a) untreated fabric, b) plasma-treated fabric

The MATLAB code is listed in Fig. 7, as seen in the script editor. The following syntax was used in our analysis: `imread(filename)` reads an image from the provided file, `rgb2gray(filename)` transforms the RGB image into a grayscale image using Eq. (5), `std2(filename)` calculates the standard deviation of each value in an array using Eq. (1), and `imhist(filename)` computes the histogram of a grayscale image using. For indicating the surface roughness of the gray image, we used Eqs. (1) to (4) to calculate the standard deviation (σ), mean (μ), standard error (SE), and coefficient of variation (CV). Our images were also created in 3-D using Meshgrid, which produces a rectangular grid of two given arrays using Cartesian indexing or matrix indexing, and `surf(X,Y,Z)`, which generates images of three-dimensional surfaces with solid edge colors and solid faces. The three-dimensional images were also created using the graph of three-variable equations, expressed as $F(x, y, z) = 0$, or we could use $z = f(x, y) = 0$.

According to SEM testing and image processing, plasma treatment reduced fabric mass with increased surface roughness, and plasma-treated fabrics had a coefficient of variation (CV) of 0.6326 higher than untreated fabrics, which is 0.5568. The higher the coefficient of variation, the greater the level of dispersion around the mean. The standard deviation of the untreated fabric is

higher than the plasma-treated fabric, this indicates that the value of pixel intensity is more dispersed in the untreated fabric. The higher pixel intensity dispersion in the untreated fabric is due to the smoother surface of the fabric compared to the plasma-treated fabric.

```

1 - I = imread('90-SEM.png'); % Load SEM image
2 - g = rgb2gray(I); % Convert to grayscale
3 - meanval = mean2(g);
4 - stdev = std2(g);
5 - stderror = stdev / sqrt(numel(g));
6 - CV = (stdev / meanval)*100; %The coefficient of mass variation CV %
7
8 - % Define pixel-to-nanometer conversion factor (replace with your own value)
9 - pixel_to_micm = 0.031; % Assuming 1 pixel = 0.031 micrometers
10
11 - [x, y] = size(g);
12 - X = 1:y;
13 - Y = 1:x;
14 - xx = X * pixel_to_micm;
15 - yy = Y * pixel_to_micm;
16 - J = double(g);
17
18 - % Display 3D surface plot
19 - figure;
20 - subplot(2, 1, 1);
21 - surf(xx, yy, J);
22 - grid on;
23 - ylabel('Position-y (micrometer)');
24 - xlabel('Position-x (micrometer)');
25 - zlabel('Intensity');
26 - colorbar;
27 - shading interp;
28 - title('Surface Roughness 3D');
29
30 - % Display original SEM image
31 - subplot(2, 1, 2);
32 - imshow(I);
33 - ylabel('Position-y (micrometer)');
34
3 usages of "I" found
    
```

Fig. 7. The MATLAB code in the script editor

Table 2. Summary of the statistical quantities of SEM images analysis

Statistical quantity	Untreated fabric	Plasma-treated fabric
Mean value (μ)	101.0185	74.8355
Coefficient of variation (CV)	0.5568	0.6326
Standard deviation (σ)	56.2469	47.3438
Standard error (SE)	1.5721	1.3233

The sensitivity of the model to interpret the roughness of the fabric surface depends on the result of the SEM image. For example, object magnification can affect the clarity of two-dimensional SEM images, which can affect the three-dimensional mapping results. It has been reported by some researchers [19, 20] that the rougher the surface of the material, the greater its surface tension and adhesion properties will be. Plasma treatment reduced the mass of ramie fabric by 0.11 %, according to our findings. We discovered that the greater the mass reduction, the greater the surface roughness value. The results of this study are also consistent with those of some other researchers who have reported the use of plasma to modify polymers, especially in terms of adhesion and roughness [22-25, 41]. Following the results of this research and the literature review, plasma treatment resulted in a decrease in fabric mass, changes in fabric surface roughness, increased surface tension and fabric adhesion, as well as an increase in hydrophilic functional groups, such as hydroxyls (O-H), carboxyls (C-O), and carbonyls (C=O). In this study, several aspects of the relationship between ramie fabric and plasma treatment in biomechanics can be understood, particularly in the context of their use in textile products and their potential in biomechanical applications. The following are the connections between ramie fabric, plasma treatment, and biomechanics: (1) Tensile strength: Ramie fabric treated with plasma has a high tensile strength due to the higher surface tension and work of adhesion of the polymers and fibers, indicating that it is able to endure pressure and tension. The tensile strength of ramie fibers can be an important consideration in the development of textile products for applications involving the

biomechanics of the human body, such as sportswear or protective equipment, in a biomechanical context; (2) Light and strong: Ramie fabric with plasma treatment has a low-density level due to a decrease in fabric mass, and changes in fabric surface roughness. Hence, the fabric is light but still strong. In biomechanical applications, the lightness and strength of ramie fabric can be useful in the development of products that not only support the body's natural movement but also provide strength and endurance; and (3) Ramie fabric absorbs moisture effectively and allows for adequate air circulation due to an increase in hydrophilic functional groups, such as hydroxyls (O-H), carboxyls (C-O), and carbonyls (C=O). Comfort is an important consideration in biomechanical product design. The ability of ramie fiber to absorb sweat and allow air to circulate can improve product comfort. The use of ramie fiber in textile products while keeping biomechanical principles in mind can result in products that are not only long-lasting but also support the physiology and movement of the human body. Because of its strength and durability, ramie fiber is a great option for use in medical products such as the dressings and bandages. Its ability to resist stress while keeping strong could be useful in these products. Natural fibers, such as ramie, may be deployed as a potential material for use in medical implants in some cases. The durability, biocompatibility, and specific strength properties of ramie fiber can be used to produce potential implant products.

4. Conclusions

This research investigated the effects of plasma treatment on the surface of nonwoven fabric made from ramie fiber using infrared spectroscopy and scanning electron microscopy (SEM). In this study, we also analyzed the relationship of surface roughness and its relationship with the chemical structure using 3-D images based on object-depth mapping (ODM) using the MATLAB® R2022a software in scanning electron microscopy (SEM). As a result of FTIR testing, nonwoven fabric exposed for six minutes almost changed compared to untreated fabric. The transmittance intensity (T%) of plasma-treated fabric was lower than that of untreated fabric. Our scanning electron microscopy (SEM) and image processing studies found that plasma-treated fabrics increased surface roughness, suggesting that their surface properties had changed. The coefficient of variation (CV) for a plasma-treated fabric was 0.6326, whereas the CV for an untreated fabric was 0.5568. Additionally, we found that plasma treatment reduced the mass of ramie fabric by 0.11 %. According to the findings, the plasma treatment in the ramie nonwoven fabric caused: 1) Nonwoven fabric became more hydrophilic, as indicated by the presence of hydrophilic chemical groups such as hydroxyl (O-H), carboxyl (O-C), and carbonyl (C=O) in the infrared spectroscopy with a deeper T%; 2) Mass reduction of nonwoven fabric was accompanied by an increase in surface roughness and work of adhesion (surface tension) via SEM testing and 3-D images based on object-depth mapping (ODM); and 3) Surface modification, the plasma-treated fabric had a coefficient of variation (CV) of 0.6326 higher than untreated fabric 0.5568. In this study, we found that MATLAB® R2022a software could generate 3-D images of surface roughness using object-depth mapping (ODM) to evaluate the physical properties of ramie fabric. Furthermore, the presence and absence of plasma treatment on ramie fabrics were studied in this research for the first time. These results will help researchers and engineers improve the properties of environmentally friendly nonwovens based on ramie.

Acknowledgements

The authors thank Universitas Gadjah Mada, Indonesia, the Industrial Human Resources Development Agency (BPSDMI), Ministry of Industry of the Republic of Indonesia and the Indonesia Endowment Funds for Education (LPDP) for providing adequate facilities and funding. We also thank our colleagues who helped us with the research and analysis.

Data availability

The datasets generated during and/or analyzed during the current study are available from the corresponding author on reasonable request.

Author contributions

Markus Paramahasti was responsible for data curation, formal analysis, investigation, software and writing the original draft paper, Valentinus Galih Vidia Putra was responsible for supervision, validation and review-editing the draft paper, and Yusril Yusuf was responsible for supervision, review the draft paper, validation and review-editing the draft paper.

Conflict of interest

The authors declare that they have no conflict of interest.

References

- [1] A. Frone, D. Panaitescu, and D. Donescu, "Some aspects concerning the isolation of cellulose micro – and nano-fibers," *UPB Scientific Bulletin, Series B: Chemistry and Materials Science*, Vol. 73, pp. 133–52, 2011.
- [2] S. K. Mahadeva, S. Yun, and J. Kim, "Flexible humidity and temperature sensor based on cellulose-polyppyrrrole nanocomposite," *Sensors and Actuators A: Physical*, Vol. 165, No. 2, pp. 194–199, Feb. 2011, <https://doi.org/10.1016/j.sna.2010.10.018>
- [3] M. A. Fuqua, S. Huo, and C. A. Ulven, "Natural fiber reinforced composites," *Polymer Reviews*, Vol. 52, No. 3, pp. 259–320, Jul. 2012, <https://doi.org/10.1080/15583724.2012.705409>
- [4] J. D. D. Melo, L. F. M. Carvalho, A. M. Medeiros, C. R. O. Souto, and C. A. Paskocimas, "A biodegradable composite material based on polyhydroxybutyrate (PHB) and carnauba fibers," *Composites Part B: Engineering*, Vol. 43, No. 7, pp. 2827–2835, Oct. 2012, <https://doi.org/10.1016/j.compositesb.2012.04.046>
- [5] Y. Xie, C. A. S. Hill, Z. Xiao, H. Militz, and C. Mai, "Silane coupling agents used for natural fiber/polymer composites: A review," *Composites Part A: Applied Science and Manufacturing*, Vol. 41, No. 7, pp. 806–819, Jul. 2010, <https://doi.org/10.1016/j.compositesa.2010.03.005>
- [6] X. Liu and L. Cheng, "Influence of plasma treatment on properties of ramie fiber and the reinforced composites," *Journal of Adhesion Science and Technology*, Vol. 31, No. 15, pp. 1723–1734, Aug. 2017, <https://doi.org/10.1080/01694243.2016.1275095>
- [7] Q. Zhang, Y. Jiang, L. Yao, Q. Jiang, and Y. Qiu, "Hydrophobic surface modification of ramie fibers by plasma-induced addition polymerization of propylene," *Journal of Adhesion Science and Technology*, Vol. 29, No. 8, pp. 691–704, Apr. 2015, <https://doi.org/10.1080/01694243.2014.997380>
- [8] C. Xu, Y. Gu, Z. Yang, M. Li, Y. Li, and Z. Zhang, "Mechanical properties of surface-treated ramie fiber fabric/epoxy resin composite fabricated by vacuum-assisted resin infusion molding with hot compaction," *Journal of Composite Materials*, Vol. 50, No. 9, pp. 1189–1198, Jun. 2015, <https://doi.org/10.1177/0021998315590259>
- [9] S. N. Pandey, "Ramie fibre: part II. Physical fibre properties. A critical appreciation of recent developments," *Textile Progress*, Vol. 39, No. 4, pp. 189–268, Dec. 2007, <https://doi.org/10.1080/00405160701706049>
- [10] A. K. Bledzki, S. Reihmane, and J. Gassan, "Properties and modification methods for vegetable fibers for natural fiber composites," *Journal of Applied Polymer Science*, Vol. 59, No. 8, pp. 1329–1336, Feb. 1996, [https://doi.org/10.1002/\(sici\)1097-4628\(19960222\)59:8<1329::aid-app17>3.0.co;2-0](https://doi.org/10.1002/(sici)1097-4628(19960222)59:8<1329::aid-app17>3.0.co;2-0)
- [11] A. K. Bledzki, S. Reihmane, and J. Gassan, "Thermoplastics Reinforced with wood fillers: a literature review," *Polymer-Plastics Technology and Engineering*, Vol. 37, No. 4, pp. 451–468, Nov. 1998, <https://doi.org/10.1080/03602559808001373>
- [12] M. Ragoubi, D. Bienaimé, S. Molina, B. George, and A. Merlin, "Impact of corona treated hemp fibres onto mechanical properties of polypropylene composites made thereof," *Industrial Crops and Products*, Vol. 31, No. 2, pp. 344–349, Mar. 2010, <https://doi.org/10.1016/j.indcrop.2009.12.004>

- [13] Y. Li, S. Moyo, Z. Ding, Z. Shan, and Y. Qiu, "Helium plasma treatment of ethanol-pretreated ramie fabrics for improving the mechanical properties of ramie/polypropylene composites," *Industrial Crops and Products*, Vol. 51, pp. 299–305, Nov. 2013, <https://doi.org/10.1016/j.indcrop.2013.09.028>
- [14] D. Ray, B. K. Sarkar, A. K. Rana, and N. R. Bose, "The mechanical properties of vinylester resin matrix composites reinforced with alkali-treated jute fibres," *Composites Part A: Applied Science and Manufacturing*, Vol. 32, No. 1, pp. 119–127, Jan. 2001, [https://doi.org/10.1016/s1359-835x\(00\)00101-9](https://doi.org/10.1016/s1359-835x(00)00101-9)
- [15] D. Ray, B. K. Sarkar, A. K. Rana, and N. R. Bose, "Effect of alkali treated jute fibres on composite properties," *Bulletin of Materials Science*, Vol. 24, No. 2, pp. 129–135, Apr. 2001, <https://doi.org/10.1007/bf02710089>
- [16] X. Li, L. G. Tabil, and S. Panigrahi, "Chemical treatments of natural fiber for use in natural fiber-reinforced composites: a review," *Journal of Polymers and the Environment*, Vol. 15, No. 1, pp. 25–33, Feb. 2007, <https://doi.org/10.1007/s10924-006-0042-3>
- [17] N. Zhou, B. Yu, J. Sun, L. Yao, and Y. Qiu, "Influence of chemical treatments on the interfacial properties of ramie fiber reinforced poly (lactic acid) (PLA) composites," *Journal of Biobased Materials and Bioenergy*, Vol. 6, No. 5, pp. 564–568, Oct. 2012, <https://doi.org/10.1166/jbmb.2012.1258>
- [18] A. K. Bledzki, A. A. Mamun, M. Lucka-Gabor, and V. S. Gutowski, "The effects of acetylation on properties of flax fibre and its polypropylene composites," *Express Polymer Letters*, Vol. 2, No. 6, pp. 413–422, Jan. 2008, <https://doi.org/10.3144/expresspolymlett.2008.50>
- [19] G. Kalaprasad et al., "Effect of fibre length and chemical modifications on the tensile properties of intimately mixed short sisal/glass hybrid fibre reinforced low density polyethylene composites," *Polymer International*, Vol. 53, No. 11, pp. 1624–1638, Aug. 2004, <https://doi.org/10.1002/pi.1453>
- [20] F. G. Torres and M. L. Cubillas, "Study of the interfacial properties of natural fibre reinforced polyethylene," *Polymer Testing*, Vol. 24, No. 6, pp. 694–698, Sep. 2005, <https://doi.org/10.1016/j.polymertesting.2005.05.004>
- [21] Y. Kusano, S. Teodoru, and C. M. Hansen, "The physical and chemical properties of plasma treated ultra-high-molecular-weight polyethylene fibers," *Surface and Coatings Technology*, Vol. 205, No. 8-9, pp. 2793–2798, Jan. 2011, <https://doi.org/10.1016/j.surfcoat.2010.10.041>
- [22] H. Rausher, M. Perucca, and G. Buyle, *Plasma Technology for Hyperfunctions Surfaces*. Weinheim, Germany: Wiley-VCH, 2010.
- [23] R. Shishoo, *Plasma Technologies for Textiles*. Woodhead Publishing Limited, 2007, <https://doi.org/10.1533/9781845692575>
- [24] R. Morent, N. de Geyter, J. Verschuren, K. de Clerck, P. Kiekens, and C. Leys, "Non-thermal plasma treatment of textiles," *Surface and Coatings Technology*, Vol. 202, No. 14, pp. 3427–3449, Apr. 2008, <https://doi.org/10.1016/j.surfcoat.2007.12.027>
- [25] M. A. Lieberman and A. J. Lichtenberg, *Principles of Plasma Discharges and Materials Processing*. New York, USA: Wiley, 2005, <https://doi.org/10.1002/0471724254>
- [26] S. Ma, V. Bromberg, L. Liu, F. D. Egitto, P. R. Chiarot, and T. J. Singler, "Low temperature plasma sintering of silver nanoparticles," *Applied Surface Science*, Vol. 293, pp. 207–215, Feb. 2014, <https://doi.org/10.1016/j.apsusc.2013.12.135>
- [27] H. Barani and A. Calvimontes, "Effects of oxygen plasma treatment on the physical and chemical properties of wool fiber surface," *Plasma Chemistry and Plasma Processing*, Vol. 34, No. 6, pp. 1291–1302, Aug. 2014, <https://doi.org/10.1007/s11090-014-9581-x>
- [28] C.-W. Kan and C.-W. M. Yuen, "Plasma technology in wool," *Textile Progress*, Vol. 39, No. 3, pp. 121–187, Dec. 2007, <https://doi.org/10.1080/00405160701628839>
- [29] K. Chi-Wai, C. Kwong, and M. Yuen Chun-Wah, "The possibility of low-temperature plasma treated wool fabric for industrial use," *AUTEX Research Journal*, Vol. 4, No. 1, pp. 37–44, Mar. 2004, <https://doi.org/10.1515/aut-2004-040107>
- [30] V. G. V. Putra and J. N. Mohamad, "Response surface methodology and artificial neural network modeling of work of adhesion on plasma-treated polyester-cotton-woven fabrics," *Journal of Adhesion Science and Technology*, Vol. 37, No. 6, pp. 976–996, Mar. 2023, <https://doi.org/10.1080/01694243.2022.2053349>
- [31] V. G. V. Putra, J. N. Mohamad, D. R. Arief, and Y. Yusuf, "Surface modification of polyester-cotton (TC 70%) fabric by corona discharged plasma with tip-cylinder electrode configuration-assisted coating carbon black conductive ink for electromagnetic shielding fabric," *Arab Journal of Basic and*

Applied Sciences, Vol. 28, No. 1, pp. 272–282, Jan. 2021, <https://doi.org/10.1080/25765299.2021.1889116>

- [32] S. F. Hamad, N. Stehling, S. A. Hayes, J. P. Foreman, and C. Rodenburg, “Exploiting plasma exposed, natural surface nanostructures in ramie fibers for polymer composite applications,” *Materials*, Vol. 12, No. 10, p. 1631, May 2019, <https://doi.org/10.3390/ma12101631>
- [33] A. C. Reddy, “Evaluation of surface roughness using image processing technique,” *International Conference on Systemics Cybernetics and Informatics*, Jan. 2004.
- [34] R. H. Neeraj and R. K. Veerasha, “A review on surface roughness measurement using image processing,” *International Journal of Research Publication and Reviews*, pp. 1104–1107, Aug. 2022, <https://doi.org/10.55248/gengpi.2022.3.8.38>
- [35] H. Zhongxiang, Z. Lei, T. Jiayu, M. Xuehong, and S. Xiaojun, “Evaluation of three-dimensional surface roughness parameters based on digital image processing,” *The International Journal of Advanced Manufacturing Technology*, Vol. 40, No. 3-4, pp. 342–348, Jan. 2009, <https://doi.org/10.1007/s00170-007-1357-5>
- [36] P. K. Gandla, V. Inturi, S. Kurra, and S. Radhika, “Evaluation of surface roughness in incremental forming using image processing based methods,” *Measurement*, Vol. 164, p. 108055, Nov. 2020, <https://doi.org/10.1016/j.measurement.2020.108055>
- [37] M. J. Thornbush, “Measuring surface roughness through the use of digital photography and image processing,” *International Journal of Geosciences*, Vol. 5, No. 5, pp. 540–554, Jan. 2014, <https://doi.org/10.4236/ijg.2014.55050>
- [38] M. Paramahasti, V. G. V. Putra, and Y. Yusuf, “An analysis of ramie fiber (*Boehmeria nivea* L. Gaud) treated with low temperature plasma using a mathematical model,” *Arab Journal of Basic and Applied Sciences*, Vol. 31, No. 1, pp. 255–264, Dec. 2024, <https://doi.org/10.1080/25765299.2024.2339556>
- [39] J. Ondra, “Measurement of roughness using image processing,” in *26th IMEKO World Congress*, 2000.
- [40] R. Kandimalla et al., “Fiber from ramie plant (*Boehmeria nivea*): A novel suture biomaterial,” *Materials Science and Engineering: C*, Vol. 62, pp. 816–822, May 2016, <https://doi.org/10.1016/j.msec.2016.02.040>



Markus Paramahasti, S.Si., M.Sc. is a doctoral student of applied physics at Universitas Gadjah Mada, Yogyakarta, Indonesia. He received his bachelor’s degree from the Department of Physics, Universitas Gadjah Mada, and a Master of Science in Theoretical Physics from Universitas Gadjah Mada in 2015 with maxima cum-laude predicate. Skills: artificial intelligence (AI), research in plasma treatment, nanotechnology, materials science, python (programming language), data science.



Assoc. Prof. Dr. **Valentinus Galih Vidia Putra**, S.Si., M.Sc., is an Associate Professor of physics at Politeknik STTT Bandung, the Ministry of Industry of the Republic of Indonesia who researches plasma, nanomaterial, and applied physics. He was born in Klaten on March 4, 1987. He received his bachelor’s degree from the Department of Physics, Universitas Gadjah Mada, in 2010. In 2012, he received a Master of Science in Applied Physics, and in 2017, a Doctor of Science in Theoretical Physics from Universitas Gadjah Mada, both with summa cum-laude predicate. Between 2017 and 2022, he researched mainly at the Department of Textile Engineering, Politeknik STTT Bandung, Indonesia.



Prof. Dr. Eng. **Yusril Yusuf**, S.Si., M.Sc., M.Eng. is a materials physicist who researches liquid crystal polymers, biomaterials, and biocomposite materials. He is best known for developing artificial muscles based on liquid crystalline elastomers. Yusril Yusuf is the founder of a research group called the Liquid Crystal Elastomers (LCE) Group. In 2006, he received the Glen Brown Award for the findings, and in 2011, he was invited to the Lindau Nobel Prize Winners Meeting. He is currently a physics professor at Gadjah Mada University (UGM) in 2021. He also received an award as the researcher with the highest publications and citations in UGM’s Outstanding People in 2021.